

Perforator Flap Magnetic Resonance Angiography for Reconstructive Breast Surgery: A Review of 25 Deep Inferior Epigastric and Gluteal Perforator Artery Flap Patients

Tiffany M. Newman, MD,^{1*} Julie Vasile, MD,² Joshua L. Levine, MD,² David T. Greenspun, MD, MSc,² Robert J. Allen, MD, APMC, FACS,² Minh-Tam Chao, BSRT(R)MR,¹ Priscilla A. Winchester, MD,¹ and Martin R. Prince, MD, PhD¹

Purpose: To evaluate the accuracy of magnetic resonance angiography (MRA) for preoperative mapping of rectus and gluteal muscle perforating arteries prior to autologous flap breast reconstruction.

Materials and Methods: Preoperative MRA on 25 consecutive patients undergoing perforator artery-based autologous breast reconstruction was performed at 1.5 T using 3D liver accelerate volume acquisition (LAVA) of abdominal or gluteal regions acquired during injection of 20 mL of gadobenate dimeglumine with bolus timing optimized using MR fluoroscopy or SmartPrep. Perforator artery size and coordinates relative to umbilicus or top of gluteal crease on 3D MRA were compared to findings at surgery. Reconstructed breast volume estimates from MRA were also compared to weights at harvesting.

Results: In all, 132 perforator arteries were found at surgery to be located within 1 cm of the coordinates measured on MRA and were surgically verified to be suitable for flap perfusion. Surgery verified the arterial course and caliber through the rectus and gluteal muscles visualized on MRA in 48 of 49 arteries. Volume rendering of 3D MRA predicted a breast reconstruction volume with a mean difference of 47 g compared to measurements at harvesting.

Conclusion: MRA accurately maps rectus and gluteal muscle perforator arteries for preoperative planning of autologous flaps for breast reconstruction.

Key Words: MRA; perforator artery; gadolinium; breast reconstruction

J. Magn. Reson. Imaging 2010;31:1176-1184.

© 2010 Wiley-Liss, Inc.

BREAST-CONSERVING SURGERY and contralateral prophylactic mastectomy after breast cancer diagnosis is increasingly utilized in treating patients with breast cancer or at high risk of breast cancer (1). Following mastectomy, new breasts may be reconstructed with a patient's own skin and fat harvested from abdominal and gluteal donor sites to create the look and feel of natural breasts without the need for future replacement. These autologous reconstructions are vascularized by perforator arteries arising from the deep inferior epigastric artery or superior/inferior gluteal arteries. Although the perforator arteries at the site of perforation are small, they are dissected down to the deep inferior epigastric artery, superior gluteal artery, or inferior gluteal artery where the diameter is large enough for anastomosis to the internal mammary or thoracodorsal arteries.

Contrary to the traditional transverse rectus-abdominus myocutaneous (TRAM) flap, muscle and fascia are spared from being cut and mobilized to form the breast, allowing for the safe transfer of viable adipose tissue from the abdomen or gluteal region vascularized by a single artery and vein bundle (2). Given the variability of the vascular anatomy and arborization patterns of perforating vessels in each individual, accurate preoperative imaging is essential in surgical planning for selection of the most favorable perforator arteries for free flap harvesting. Preoperative imaging can improve patient care by providing the surgeon with precise localization of vessels to reduce dissection times, shorten anesthesia time, and decrease the likelihood of surgical complications (3,4).

¹Department of Radiology, Weill Cornell Imaging at New York Presbyterian, New York, New York, USA.

²Center for Microsurgical Breast Reconstruction, New York, New York, USA.

*Address reprint requests to: T.M.N., Radiology Department at NYPH-WCMC, 416 East 55th Street, New York, NY 10022. E-mail: tin9004@nyp.org

Received June 15, 2009; Accepted February 2, 2010.

DOI 10.1002/jmri.22136

Published online in Wiley InterScience (www.interscience.wiley.com).

Magnetic resonance angiography (MRA) has been used in autologous transplants to evaluate the vascular anatomy of lower limbs for fibular free flap harvesting in mandibular reconstruction (5). The approach of MRA over conventional angiography is well supported because MRA has the advantage of no radiation, multiplanar capability, safer contrast agents, and lack of invasiveness while providing detailed vascular mapping and estimates of flap volumes from various donor sites (5). MRA is beginning to be explored as an alternative to computed tomography angiography (CTA) in mapping perforator arteries where MRA has the advantages of no ionizing radiation and fewer contrast reactions. MR has been studied for the preoperative mapping of rectus muscle perforators at 3 T with promising results (6,7). There is no study that looks at MRA use in evaluating rectus and gluteal muscle perforators for this type of flap procedure. In this study we employed MRA at 1.5 T using fat-suppressed 3D spoiled gradient echo, parallel imaging in both rectus and gluteal perforator artery flap planning for breast reconstruction, in addition to preoperative estimation of reconstructed breast volumes. The purpose of this study was to evaluate the accuracy of MRA with postprocessing 3D reconstruction for the preoperative mapping of abdominal and gluteal perforating vessels and flap volume estimation.

PATIENTS AND METHODS

Patients

We conducted this Institutional Review Board (IRB)-approved study of 25 consecutive patients undergoing preoperative MRA between August 1, 2008 to May 31, 2009 followed by perforator-based autologous tissue breast reconstruction. Because these studies were part of the patients' routine clinical care and analyzed retrospectively, informed consent was not required. The patients were 32–60 years old, mean age 44 years. All patients presented to the Center for Microsurgical Breast Reconstruction for breast reconstruction following mastectomy ($n = 5$), lumpectomy ($n = 1$), breast cancer diagnosis but prior to surgery ($n = 18$), or with noncancerous breast disease ($n = 1$). They were evaluated for suitability of breast reconstruction with autologous tissue transfer from abdominal or gluteal donor sites. Those women who were candidates for abdominal or gluteal flap-based reconstruction were then sent for preoperative MRA.

MRI Technique

All patients were scanned at 1.5 T (GE Signa HDx 14.0, Waukesha, WI) using the body coil for transmission and 8-channel body ($n = 19$) or 8-channel cardiac ($n = 6$) phased array coils for reception.

The coils were chosen by a radiologist based on size of patient and area of interest (abdomen only, abdomen and pelvis, or pelvis and upper thigh region) to be evaluated. A 3D liver accelerate volume acquisition (LAVA) sequence was acquired from 3 cm above the

patient's umbilicus down to the upper thigh using 3-mm slice thickness zero padded to a 1.5-mm slice spacing. The acquisition matrix was $512 \times 192 \times 256$. The field of view ranged from 44–48 cm. Voxel dimensions were $3 \times 1.9\text{--}2.3 \times 0.9$ mm. The length of breath hold after deep inspiration was about 30–35 seconds per acquisition. Breath holding was achieved in all patients after hyperventilation (typically two preceding cycles of maximum inspiration and maximum expiration). Axial LAVA sequences with 2-fold parallel imaging and fat suppression were acquired before (precontrast), during (dynamic arterial phase), and after administration of intravenous (IV) gadolinium with the following parameters: TR/TE/flip = 4.1/1.9/15, bandwidth = 100k Hz to 125k Hz, NEX = 0.71. The injection consisted of 20 cc of gadobenate dimeglumine, followed by 20 cc of normal saline at the rate of 1.5–2 cc per second. The first axial LAVA sequence started 4 seconds after observing gadolinium arriving in the abdominal aorta on MR fluoroscopy ($n = 13$) or detection by SmartPrep ($n = 12$). k -Space was mapped sequentially so the center of k -space typically occurred 15–20 seconds after initiating scanning. After arterial phase imaging was obtained, delayed contrast-enhanced imaging was performed in the coronal plane with an acquisition matrix of 512×256 , the sagittal plane with a matrix of 512×224 , and another "high resolution" axial plane with a matrix of 512×512 . In the sagittal plane the slice thickness was increased to 4.0 mm to maintain breath hold times less than 40 seconds. High-resolution, delayed enhancement axial images were acquired during free breathing (Fig. 1). All images were postprocessed on

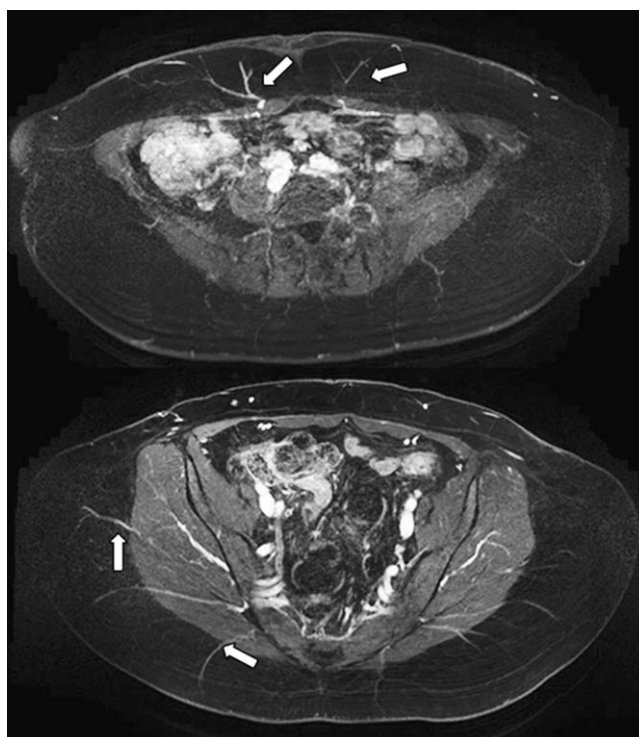


Figure 1. High-resolution (512×512), free breathing axial LAVA images through the abdomen (top) and gluteal (bottom) regions shows several perforator arteries (arrows).



Figure 2. Photograph of buttock with marker at top of gluteal crease (arrow).

an Advantage Workstation using maximum intensity projections and volume rendering.

Initial Protocol

In the first two patients, positioning was supine initially and then prone for additional delayed imaging.

There were inconsistencies with operative reports of perforator vessel coordinates due to 1) shifting of the abdominal wall resulting in motion artifact that made it difficult to measure from a distinct reference point (umbilicus); 2) measuring diameter in mixed arterial and venous phases, causing surgeon's to believe arteries were larger than they actually were; and 3) measurements of gluteal coordinates with an unnatural buttock contour from supine positioning. These patients were not included in the final analysis.

Standardized Protocol

In the next 23 patients (mean age 44 years; range 32–62), the protocol was standardized as follows.

The patients were all placed prone first on viscoelastic foam, 2 inches thick, with the top of the gluteal crease utilized as the landmark/coil center as well as reference point for measurement of gluteal artery coordinates (Fig. 2). The axial LAVA images were obtained pre- and postcontrast in addition to a LAVA sequence in the coronal plane. The prone position minimized anterior abdominal wall motion, thereby improving rectus muscle perforator assessment while maintaining gluteal contour to assess gluteal muscle perforators. The patient was then placed in the supine position with a landmark at the center of the coil. The umbilical insertion into the fascia was then used as a reference point for measuring rectus muscle perforator artery coordinates. In this supine position, axial

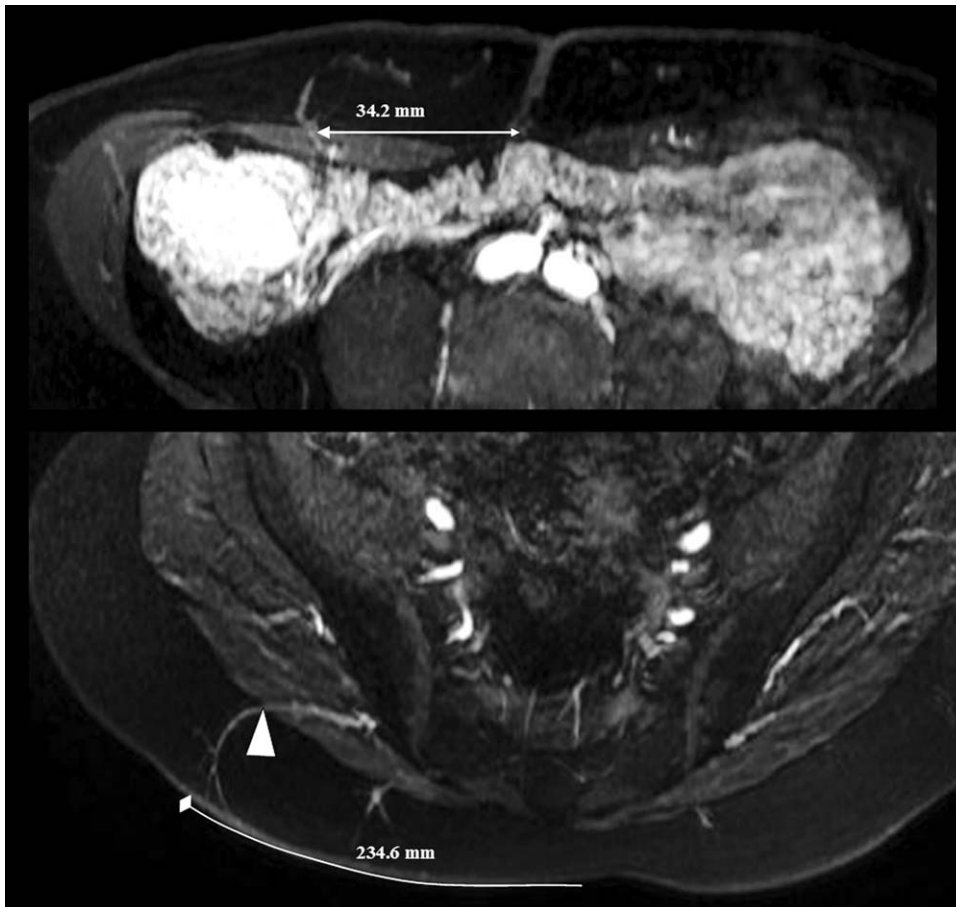


Figure 3. MRA (axial view). Arterial phase of rectus muscle perforator (white double arrow). Double arrow shows distance between umbilicus and site of perforation through rectus muscle fascia (top). MRA (axial view) 2.4 mm gluteal artery perforator (arrowhead). Curved white line along skin surface reveals the measured horizontal distance (234.6 mm) from a midline that corresponds to a vertical line extending from the top of the gluteal crease landmark. The lateral most endpoint (diamond) is where the surgeon places the Doppler probe and skin marking to confirm perforator artery location prior to dissection (bottom).

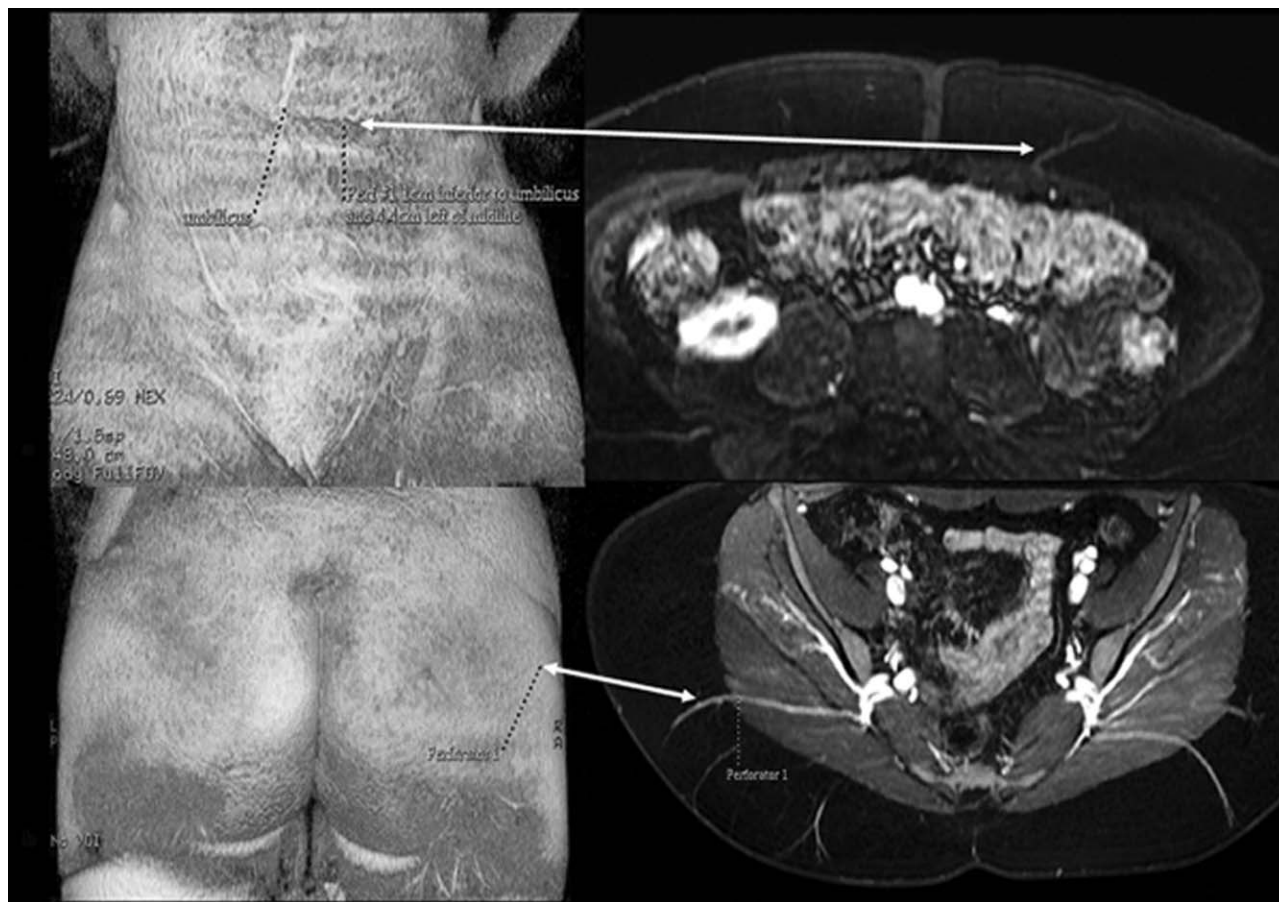


Figure 4. Perforator artery perforation sites identified on axial LAVA arterial phase imaging are displayed on 3D surface renderings of the abdomen (top) and pelvis (bottom) (double arrows) to guide flap planning and surgical dissection.

and sagittal LAVA images were obtained. These supine axial images enabled measurement of abdominal subcutaneous tissue volume without the effect of compression on the surface of the patient's abdomen.

Average total time for completion of the MRI using the standardized protocol was 40 minutes. The minimum time for completion of the MRA protocol was 30 minutes for area-specific studies, ie, imaging for solely gluteal muscle or rectus muscle perforators. Maximum time to completion of the protocol when both gluteal and rectus muscle perforators need to be visualized (larger craniocaudal distance) was 45 minutes.

Image Postprocessing and Interpretation

Three dimensional surface-rendering of the images was generated on a workstation (Advantage Windows, GE Medical Systems, Waukesha, WI). The rectus and gluteal muscle perforator artery sites of perforation through the superficial muscle fascia were determined using axial LAVA images in the arterial phase and measured relative to insertion of the umbilicus into the fascia and top of gluteal crease, respectively (Fig. 3). Coordinates identifying the location of the perforating arteries on the 3D reconstructed surface were displayed on surface rendered images (Fig. 4). These coordinates and images were used by surgeons

to locate perforator arteries intraoperatively. A radiologist measured perforator artery diameters at the site of penetration through the rectus muscle and fascia using the Advantage Workstation. The supine images were utilized to estimate flap volumes by designing the flap on the volume rendered image and calculating the flap volume (Fig. 5). The standard flap extended from 2 cm above the umbilicus down to the pannus crease at the pubic symphysis. In the left-right direction it extended to the mid-axillary lines bilaterally at the level of the iliac crests. Surgical findings with respect to relative perforator size, location, and course were recorded.

Surgical Correlation

The day prior to surgery, a plastic surgeon reviewed the MRA images and selected the perforators suitable for harvesting. The surgeon then premarked the primary and back-up perforator arteries on the patient's skin at the locations described in the MRA report using a metric ruler and a marking pen. The presence of each marked perforator artery locations was assessed with a handheld Doppler probe. At surgery, the surgeons reconfirmed perforator location with a handheld Doppler prior to dissection, then began surgical dissection of all rectus muscle perforator arteries (since the entire abdominal wall is dissected

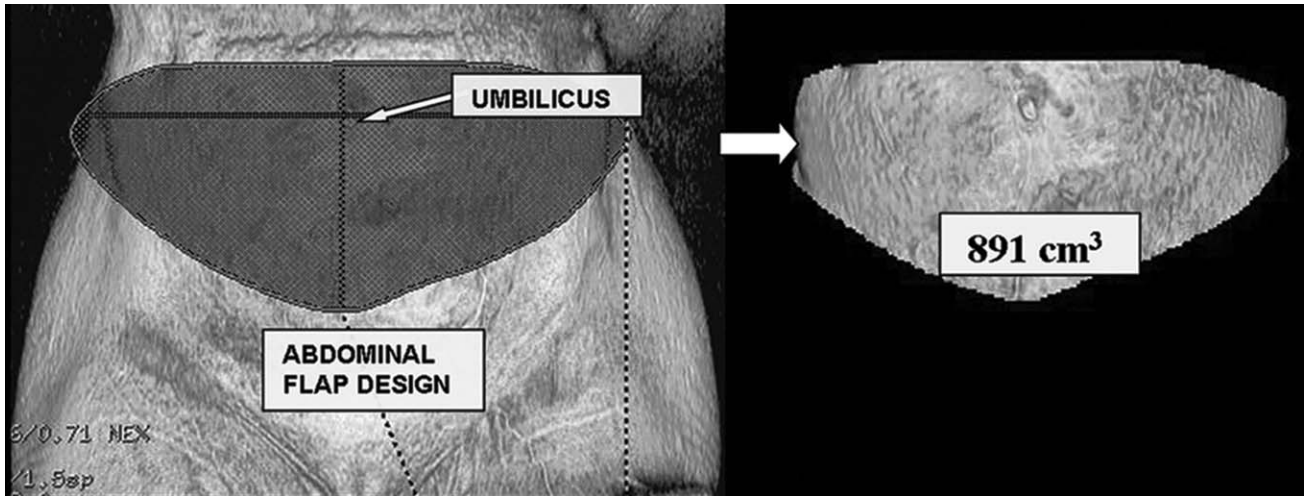


Figure 5. Three-dimensional volume rendering of a supine axial LAVA image is utilized to design flap. For abdominal perforator-based flaps, the entire abdomen below umbilicus is dissected and removed, therefore the surgeon is able to confirm all perforator artery locations reported (left). Simulated flap harvesting on the computer (right) is used to estimate flap volume.

routinely), but only the primary and backup gluteal perforator arteries (as the surgeons only utilize a small area of the gluteal region for the flap) (Fig. 6). Thus, surgical correlation was available for all rectus perforator arteries and for primary and back up gluteal perforator arteries (Fig. 7). A flap volume measurement at the time of surgery was done during harvesting of the flap tissue. After the subcutaneous fat was dissected off of the rectus fascia and the perforator vessels were isolated and cut, the total abdominal free flap was weighed.

RESULTS

Perforator flap MRA was performed successfully in all 23 patients of the standardized exam group. No patient declined the exam for claustrophobia or any other reason. One additional patient with a breast tissue expander had CTA, although we subsequently realized that this was not a contraindication to MRA. In one patient a superficial thrombophlebitis occurred at the intravenous injection site 2 days postgadobenate dimeglumine injection in spite of flushing with 20 mL normal saline. There were no other adverse reactions to gadolinium.

Early Group

In the first two patients we noted that when the patient was supine, image quality was degraded by motion with blurring of the anterior abdominal wall in spite of breath holding. The subsequent patients were imaged in the prone position for the arterial and mixed arterial-venous phases, in addition to coronal and high-resolution axial LAVA images. Prone positioning minimized anterior wall motion during the arterial phase when breath holding was not perfect or if the patient was moving in spite of breath holding. Patients were then rotated to the supine position for axial and sagittal LAVA images. Having both

prone and supine views gave more information on skin contours so anterior abdominal wall flap volumes could be measured without distortion from prone positioning.

Early feedback from surgeons revealed perforator locations identified at time of surgery were still greater than 1 cm off from the coordinates given on MRA using prone positioning to derive measurements. This discrepancy was attributed to using skin position of the patient's umbilicus as a reference point as opposed to the point at which the umbilicus enters the fascia; the latter generating results that compared well with intraoperative findings (Fig. 7). Although perforators were best visualized on mixed arterial-venous phase images, the perforator size measurement

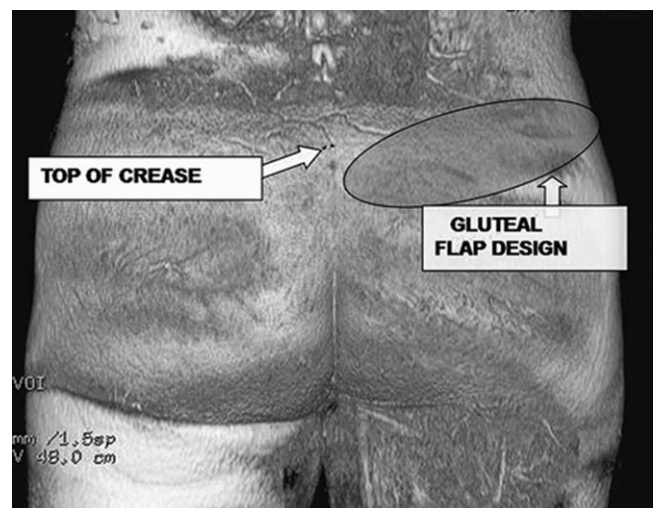


Figure 6. Three-dimensional volume rendering of a prone axial LAVA image is utilized to design gluteal flap. This illustrates why the surgeons can only confirm location of primary and back-up arteries during a gluteal flap-based reconstructive surgery due to the limited area of tissue that is dissected and removed from the body.

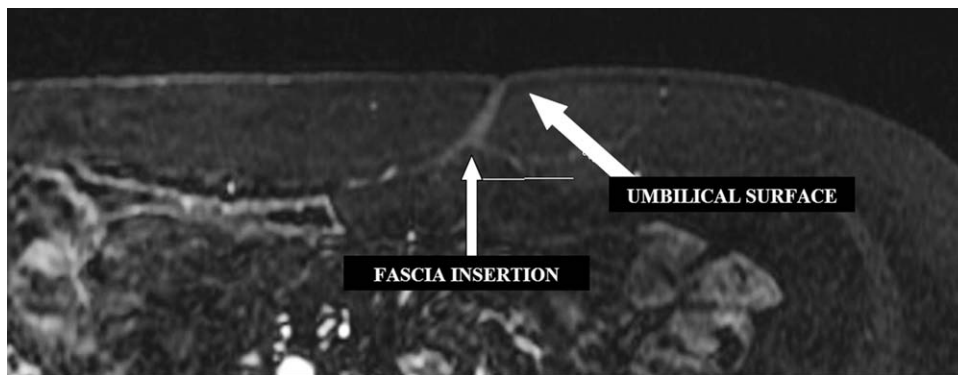


Figure 7. Axial LAVA image demonstrating the shift in umbilical surface (thick arrow) compared to the fascia insertion (thin arrow) of umbilicus when patient is prone.

correlated more closely on pure arterial phase axial LAVA images.

Standardized Exam Diameter and Location Determination

In the next 23 patients perforator artery diameter on MRA was visually estimated within 1 mm by the surgeon to be correct for 130 of 132 dissected arteries. In one deep inferior epigastric perforator flap, however, the perforator artery chosen on the basis of MRA, measuring 1.7 mm diameter, was not used because at surgery another perforator artery measured on MRA to be 1.4 mm in diameter actually appeared larger after surgical dissection. The mean size of all arterial diameters measured on MRA was 1.8 mm (range: 0.9–2.9 mm) for rectus muscle perforators (visualized at surgery) and 1.7 mm (range: 1.3–4.2 mm) for gluteal muscle perforators.

For these 23 patients perforator artery location was verified surgically to be within 1 cm of MRA coordinates for all 132 dissected arteries (sensitivity = 99%).

There was one false-negative (sensitivity = 99%). MRA failed to report one artery found at time of surgery that was a small rectus abdominus perforator. At surgery, the large vein associated with this perforator was used, but the corresponding perforator artery was considered to be too small to support the graft. Although in retrospect this perforator artery was visible on MRA, it was not reported because it was thought to be too small. There were no false-positives, ie, no MRA-reported vessels not seen at the time of surgery (specificity = 100%). In 16 of 23 cases (69%), surgeons shifted the standard flap design more cephalad, caudal, or lateral extension after reviewing MRA to incorporate MRA-reported perforators they found to be suitable for supporting the free flap (Table 1). All gluteal ($n = 3$) and 13 abdominal flaps were modified by position and/or shape after reviewing MRA.

Standardized Exam Intramuscular Course Determination

Of the 132 arteries dissected, there were 49 perforator arteries described by MRA that were harvested and utilized for supporting 40 free flaps (bilateral flap = 16 or 32 hemi-flaps; unilateral = 8). In nine cases the

flap was supported by two or more perforator arteries because they joined together prior to joining the deep inferior epigastric or gluteal arteries. Thirty-nine of the 40 flaps were successful. One deep inferior epigastric artery perforator-based flap failed secondary to arterial thrombosis; however, was successfully replaced with another autologous flap. All 49 arteries were dissected down to either the deep inferior epigastric artery ($n = 42$), superior gluteal artery ($n = 4$), or inferior gluteal artery ($n = 3$). For 48 of these 49 perforator arteries the MRA determined intramuscular course was verified to be correct. For the one remaining artery, MRA showed a transverse course anterior to the rectus muscle; however, at surgery the artery was actually within the anterior surface of the muscle as it traversed horizontally requiring a larger muscle dissection than had been anticipated.

Standardized Exam Flap Volume Estimation

Data on MRA flap volume measurements compared to intraoperative flap weights are shown in Table 2 with a mean difference of 47 g.

Flap Outcomes

In all but one case, flaps were successfully transferred on the vessels the surgeon selected based on MRA. In the patient who had superficial thrombophlebitis at the gadobenate dimeglumine injection site, one transplanted perforator artery thrombosed on postoperative day 1 and despite multiple attempts the flap was not salvageable. A superior gluteal artery perforating branch previously identified and reported on MRA was utilized and successfully supported a replacement flap.

DISCUSSION

More women are choosing to undergo immediate autologous breast reconstruction at the same time of mastectomy, as the procedure offers excellent cosmetic outcome and has proven to be safe in breast cancer patients (1,8). Additionally, this procedure offers the advantage of improved disease-free survival while providing aesthetic outcomes (9). The conventional transverse rectus-abdominis myocutaneous (TRAM) flap has been used since its introduction in 1982 by

Table 1
Changes in Surgical Plan Due to MRA

Patient	Flap type	Surgeon changes in flap design from MRA data
1	DIEP-bil ^{a,b}	Shifted flap superiorly to capture and center around perforator artery 2 cm above umbilicus
2	DIEP-uni ^c	No change
3	DIEP-uni	Flap shifted inferiorly for better aesthetics and to capture larger perforator.
4	IGAP-bil ^d	Flap designed flap around the 4th perforator artery described, which was more lateral to obtain more subcutaneous tissue closer to that perforator
5	DIEP-bil	No change
6	DIEP-uni	Flap shifted upward to capture paraumbilical perforators
7	DIEP-bil	No change
8	DIEP-bil	Flap shifted upward to capture umbilical perforator
9	DIEP-bil	Flap shifted to utilize perforator artery close to umbilicus on left
10	SGAP-uni ^d / DIEP-uni (hemi-flap failed)	No change for DIEP flap; SGAP flap shifted superiorly to center around 2 adjacent preselected perforator arteries
11	DIEP-uni	Flap created around inferior perforator to design a low scar
12	DIEP-bil	No change
13	DIEP-bil	Flap shifted superiorly to capture periumbilical perforator artery
14	DIEP-uni	MRA made surgeon aware of small perforators, thus flap shifted inferiorly to utilize the superficial inferior epigastric artery and vein system
15	DIEP-bil	Flap shifted superiorly to capture right periumbilical perforator
16	DIEP-bil	Flap extended superiorly to capture periumbilical perforator
17	DIEP-bil	A more superior flap design created to capture 2 joining left perforators.
18	DIEP-bil	No change
19	DIEP-bil	No change
20	DIEP-uni	Flap shifted to upward capture perforator superior to umbilicus
21	DIEP-bil	Flap shifted superiorly to capture perforators that joined in the periumbilical area.
22	DIEP-bil	No change
23	SGAP-bil	Flap moved upward off of buttock, toward lower back region

^aDeep inferior epigastric artery perforator.

^bBil, bilateral abdominal or gluteal flap.

^cUni, unilateral abdominal or gluteal flap.

^dInferior or superior gluteal artery perforator.

Hartampf et al (10). However, a recent refinement is to harvest just the skin and fat together with a supporting perforator artery so the rectus abdominus muscle and fascia are spared. Advantages of the perforator artery-based flap refinement (ie, deep inferior epigastric artery, superior gluteal artery or inferior

gluteal artery) compared to conventional TRAM flaps include: reduced rectus muscle dissection with most of its anterior sheath left intact to maintain the strength and integrity of the abdominal wall, reduced donor site pain, decreased rate of hernias, and shorter recovery times (11). This type of procedure benefits from preoperative mapping of the vascular anatomy to plan the details of the surgery and has primarily been performed utilizing Doppler ultrasound and CTA (2,4,12). However, ultrasound and CTA have several limitations. Doppler ultrasound limitations include 1) inability to distinguish perforators that arise from the superficial or deep system; 2) failure to accurately locate perforators that do not exit fascia perpendicularly; 3) inability to differentiate large from small perforator arteries; and 4) inability to map anatomic vessel course through the rectus abdominus or gluteal muscles (12). As a result, there have been significant inconsistencies with high false-positive and false-negative rates when Doppler ultrasound is compared with intraoperative findings (12–14). Although CTA has good spatial resolution and is highly sensitive (100%) and specific (100%) for precise preoperative detection of perforator location when compared with Doppler ultrasound, it has the limitation of ionizing radiation exposure (14). Some women with breast cancer may be sensitive to the use of CTA since they typically undergo extensive imaging for work-up as well as for posttreatment procedures and surveillance

Table 2
MRA Flap Volume Estimation

Patient	Flap volume measurements		
	MRA (cm ³)	Surgery (g)	Difference ^a
1	652	605	47
2	641	643	2
3	482	464	18
4	N/A	986 ^b	N/A
5	411	444	33
6	891	908	17
7	894	869	25
8	1011	1084	73
9	1407	1420	13
10	1406	1460	54
11	810	758	52
12	1718	1736	18
13	653	616	37
14	234	176	58
15	1353	1242	111
16	1260	1144	116
17	1085	1077	8
18	1105	1073	32
19	2494	2550	56
20	880	910	30
21	1267	1292	25
22	802	982	180
23	N/A	1106 ^b	N/A
Mean	1022 cm ³	1021	47g
SD	500	517	43

^aAssuming a mean density of all flap components (fat tissue, blood vessels, skin) is 1 g/cm³. Difference = MRA volume in cm³ * (1g/cm³) – weight at surgery.

^bNot included in calculation.

(ie, mammography, CT, chest radiography, PET CT, etc) that involves the use of ionizing radiation. Thus, the use of high-resolution CTA for preoperative mapping of perforator vessels becomes yet another exposure for these patients, which is negatively viewed as more and more studies report links between radiation exposure and cancer (15).

This study of 23 standard protocol patients undergoing breast reconstruction demonstrates the high sensitivity and specificity of MRA with surgical confirmation in identifying precise location of abdominal wall and gluteal perforator arteries of sufficient caliber to support autologous flaps: 99% and 100%, respectively. The sensitivity and specificity of MRA precision in identifying perforator coordinates are considerably close in comparison to those of CTA; however, a comparative study would be useful. A recent article by Greenspun et al (16) commented on the difference in our technique from their original abdominal perforator MRI protocol in that the images rendered demonstrate improved spatial resolution and sufficient fat suppression to reliably visualize lateral row abdominal perforators, an effort to reduce the number of false-negatives. MRA allowed surgeon's to identify arterial perforators with varying characteristics, of which the largest arterial diameters and minimal intramuscular course were considered most desirable as these factors would be most suitable for supporting flaps as well as facilitating dissection. Septocutaneous arteries, which are arteries that travel around rectus muscle or between gluteal muscles along fascial planes and have no intramuscular course, are also highly desired. Perforator artery detail was demonstrated during postprocessing by displaying their specific branching patterns into the subcutaneous tissue as well as the perforator artery course as it arose from the deep inferior epigastric artery, superior gluteal artery, or inferior gluteal artery. This in addition to the high percentage (69%) of flap designs changed after reviewing the MRA supports our hypothesis that the surgeon's preoperative decision-making was greatly enhanced.

Positioning

Prone positioning during dynamic arterial phase imaging enabled assessment of both rectus and gluteal muscle perforator arteries in the same acquisition. The natural contour of the gluteal region captured during prone positioning was necessary for accurate measurements of gluteal artery perforator relationship to skin. Using 2 inches of viscoelastic foam preserved the anterior abdominal wall contour sufficiently for perforator assessment in the prone position but anterior wall flap volume was more accurate from supine data.

Limitations

MRA still has some important limitations. On some images we were unable to adequately differentiate between the fascia-muscle borders. If a vessel is identified right beneath the fascia with high signal inten-

sity postcontrast, we may not be able to predict whether or not the vessel is embedded within the superior portion of the muscle versus traveling beneath the fascia. The location of perforation through the fascia, however, is not compromised in this situation as the surgeon can readily visualize the artery through the fascia. MRA is not available in patients with pacemakers or other contraindications to MRI. MRA requires more time than CTA for data acquisition and has lower resolution. One reason MRA takes more time is because images are acquired both prone and supine for a more comprehensive assessment of how arteries relate to the contours of the flesh in different positions. This is not practical with CTA due to the extra radiation exposure required. Advances in MR technology with larger arrays of smaller coils and higher relaxivity contrast agents are likely to enhance the resolution of MRA in the future (17). Refinements to our protocol at 3 T to improve fat suppression and reduce artifacts may allow use of higher field strength to increase the signal-to-noise ratio and image quality as well.

In conclusion, 1.5 T MRA safely and accurately images the vascular anatomy of the abdominal wall and gluteal regions for use in guiding autologous flap harvesting.

ACKNOWLEDGMENT

The authors thank Dr. Martin R. Prince MD, PhD, for help with article editing.

REFERENCES

1. Tuttle TM, Habermann EB, Grund EH, Morris TJ, Virnig BA. Increasing use of contralateral prophylactic mastectomy for breast cancer patients: A trend toward more aggressive surgical treatment. *J Clin Oncol* 2007;25:5203-5209.
2. Granzow JW, Levine JL, Chiu ES, Allen RJ. Breast reconstruction with the deep inferior epigastric perforator flap: history and an update on current technique. *J Plast Reconstr Aesthet Surg* 2006;59:571-579.
3. Alonso-Burgos A, Garcia-Tutor E, Bastarrika G, Cano D, Martinez-Cuesta A, Pina L. Preoperative planning of deep inferior epigastric artery perforator flap reconstruction with multislice-CT angiography: imaging findings and initial experience. *J Plast Reconstr Aesthet Surg* 2006;59:585-593.
4. Giunta RE, Giesweid A, Feller AM. The value of preoperative Doppler sonography for planning free perforator flap. *Plast Reconstr Surg* 2000;105:2381-2386.
5. Kelly AM, Cronin P, Hussain HK, Lony FJ, Chepeha DB, Carlos RC. Preoperative MR Angiography in free fibula flap transfer for head and neck cancer: Clinical application and influence on surgical decision making. *AJR Am J Roentgenol* 2007;188:268-274.
6. Chernyak V, Rozenblit AM, Greenspun DT, et al. Breast reconstruction with deep inferior epigastric artery perforator flap: 3.0-T gadolinium-enhanced MR imaging for preoperative localization of abdominal wall perforators. *Radiology* 2009;250:417-424.
7. Neil-Dwyer JG, Ludman CN, Shaverien M, McCulley SJ, Perks AGB. Magnetic resonance angiography in preoperative planning of deep inferior epigastric artery perforator flaps. *J Plast Reconstr Aesthet Surg* 2009;62:1661-1665.
8. Cocquyt V, Blondeel P, Depypere HT, et al. Better cosmetic results and comparable quality of life after skin-sparing mastectomy and immediate autologous breast reconstruction compared to breast conservative treatment. *Br J Plast Surg* 2003;56:462-470.
9. Nold RJ, Beamer RL, Helmer S, McBoyle MF. Factors influencing a woman's choice to undergo breast-conserving surgery versus modified radical mastectomy. *Am J Surg* 2000;180:413-418.

10. Hartrampf C, Schefflan F, Black PW. Breast reconstruction with a transverse abdominal island flap. *Plast Reconstr Surg* 1982;69:216-225.
11. Ramakrishnan V, Tare M. Post-mastectomy breast reconstruction: microsurgical methods. *Indian J Plast Surg* 2007;40:82-89.
12. Rozen WM, Phillips TJ, Ashton M. Preoperative imaging for deep inferior epigastric artery perforator flaps a comparative study of computed tomographic angiography and Doppler ultrasound. *Plast Reconstr Surg* 2008;121:9-16.
13. Masia J, Clavero JA, Larranaga JR, Alomar X, Pons G, Serret P. Multidetector-row computed tomography in the planning of abdominal perforator flaps. *J Plast Reconstr Aesthet Surg* 2006;59:594-599.
14. Rozen WM, Phillips TJ, Ashton MW, Stella DL, Gibson RN, Taylor GI. Preoperative imaging for DIEA perforator flaps: a comparative study of computed tomographic angiography and Doppler ultrasound. *J Plast Reconstr Surg* 2008;121:9-16.
15. Brenner DJ, Hall EJ. Computed tomography—an increasing source of radiation exposure. *N Engl J Med* 2007;357:2277-2284.
16. Greenspun D, Vasile J, Levine JL, et al. Anatomic imaging of abdominal perforator flaps without ionizing radiation: seeing is believing with magnetic resonance imaging angiography. *J Reconstr Microsurg* 2010;26:37-44.
17. Goyen M, Shamsi K, Schoenberg SO. Vasovist-enhanced MR angiography. *Eur Radiol* 2006;16(Suppl 2):B9-14.